Design and Analysis of an Integrated Cuk-SEPIC Converter with MPPT for Standalone Wind/PV Hybrid System

Kumar. K[*], Ramesh Babu. N [**‡], Prabhu. K.R [***]

[*]School of Electrical Engineering, VIT University, Vellore, India

[**]School of Electrical Engineering, VIT University, Vellore, India

[***]School of Electrical Engineering, VIT University, Vellore, India

(kumar3kk@gmail.com , nrameshbabu@vit.ac.in, prabhu.kr@vit.ac.in)

‡ Corresponding Author; Second Author, VIT University, Vellore, India, Tel: +91 416 2202467,

Fax: +91 416 2243092, nrameshbabu@vit.ac.in

Received: 26.08.2016 Accepted:14.11.2016

Abstract- This paper proposes an integrated Cuk-SEPIC converter for standalone hybrid wind and photo voltaic (PV) system. The proposed converter is developed by sharing the converter components between Cuk and SEPIC converters and it operates in both individual and simultaneous modes, based on the availability of source and eliminates the need of input filter to suppress the high frequency harmonics. Therefore, it has the advantage of simple structure and reduced converter components. The proposed converter is designed and then analyzed for the hybrid wind and PV system. This study considers a 1.8 KW wind system and a 2 KW PV system with maximum power point tracking (MPPT) algorithms of incremental conductance plus integral control and perturbs & observes methods for wind and PV system respectively. The effectiveness of the proposed converter is validated using the simulation results and usage of the converter is based on availability of the renewable energy sources is presented.

Keywords Photo Voltaic, Wind energy, hybrid energy system, Cuk-SEPIC converter, MPPT.

1. Introduction

Electrical energy plays an essential role in human day to day life and its utilization decides the standard of living. As a result, the demand of power increases rapidly and the fossil fuels are the major sources for its generation. The main disadvantages of these sources are exhaustible in nature, causes serious environmental pollution and its utilization also crosses its limits, and expected to be exhausted in the next few decades. So, renewable energy sources are considered as an alternative energy sources to meet the load demand. At present, research in electricity generation is geared up towards the renewable energy sources (RES) due to inexhaustible in nature, pollution free and abundant presence.

The main drawbacks of RES are uncontrollable and unpredictable in nature. Thus it is difficult to generate require quantity of power to meet the load demand and also the generated power contain a lot of variations in frequency and voltage [1]. The above problems are solvable by integrating two or more renewable energy sources along with a storage system. Mostly solar and wind energy sources are integrated together because of its abundance in nature and both are complement to each other to a certain extent [1]. Usually in sunny days no wind occurs and strong winds are often occurring on cloudy days or during night time. So that, when one of the sources is unavailable or insufficient to meet the load demand, then another source will compensate the difference and meets the load demand. For such integration, the system requires power electronic converters to enhance the power transfer efficiency and to ensure reliability of the system.

In hybrid power generation system, different types of power electronic converters (PEC) are used for integration of diverse energy sources. The possible configurations of hybrid systems are mainly AC shunt coupled, DC shunt coupled and hybrid coupled systems [2]. For wind generation system, back-to-back AC/DC/AC converter is used and for PV system boost converter along with inverter is utilized. If both PV and wind sources are integrated together, then the system utilizes independent PEC by integrating some component of converters to hence reduce around 25% of power semiconductor switches [1].

Generally, two separated inverters are used for the grid integration of hybrid energy sources by common AC shunted method, this can be modified by single common inverter by integrating hybrid energy sources by common DC shunted method and this can be further modified by introducing multi input converter for integration of hybrid energy sources and an inverter for grid integration [2].

Many DC-DC converter topologies are proposed for integration of different energy sources in recent years [3-5]. Hybrid renewable energy system injects high frequency current harmonics into the system. This may increase the heating issues and decreases the generator lifespan and efficiency of the system. This cannot be eliminated by the common DC-DC converter. So it requires separate input passive filters to reduce this harmonic content, which increases the cost and makes the bulky system.

In this paper, a new converter topology of integrated Cuk-SEPIC is proposed for integration of wind and PV system. The advantage of the proposed converter is to eliminate the necessity of input filters to reduce the high frequency harmonics and it will operate in both individual and simultaneous modes of operation. The PV energy system is regulated by the Cuk converter with perturb and observer method to extract maximum power and wind energy system is regulated by the SEPIC converter with incremental conductance plus integral control to extract maximum power.

The major advantage of the proposed system is when one of the sources is not available and then the other source will supply the necessary power to meet the load demand. Due to the alternative nature of sources, the average output voltage of the hybrid system is the sum of PV and wind output voltages.

This paper is organized as follows. In section 2, design and analysis of proposed Cuk-SEPIC converter is discussed. In section 3, power conversion analysis and operation of closed loop system are discussed. Finally the implementation results are discussed in section 4.

2. Design and Analysis of Proposed System

2.1. PV array

The solar cell is an electrical device, formed by the p-n junction of semiconductor material. It converts available solar irradiations directly into the electrical energy by the photovoltaic effect. PV panel is formed by connecting numbers of solar cells in series and parallel to meet the rated voltage and current of application. The Fig. 1 shows the equivalent circuit and symbol of the solar cell [6,7].

The mathematical modeling of the solar cell is done by the V-I relationship of the PV system and current of a PV panel is a function of the solar irradiation and temperature of the panel and it is determined [6,7] by using Eq. (1),

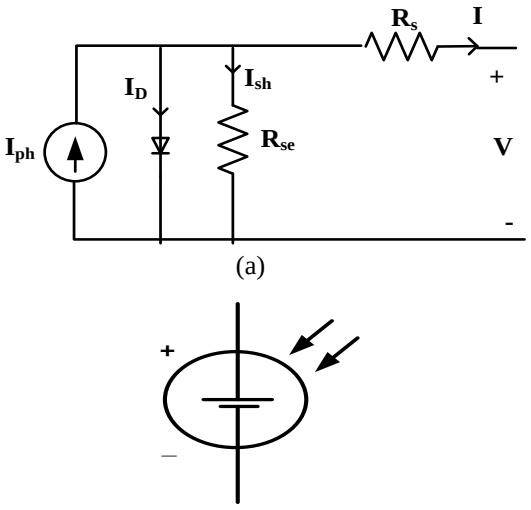

Fig. 1 Solar cell, (a) Equivalent circuit, (b) symbol

$$I_{PV} = I_{Ph} - I_P\left(e^{\frac{q\left(v_{PV}+i\,R_S\right)}{NsKT}}\right) - \frac{v_{PV}+i\,R_S}{R_{Sh}} \qquad (1)$$

where:

I_{PV}: PV panel current (A), i: current of PV cells at the output terminals (A), V_{pv}: voltage of PV cells at the output terminals (V), I_p: current in series resistor (A), I_{Ph}: photocurrent (A), K: Boltzman constant (1.38 *10-23 J/K), T: Ambient temperature (K), R_s and R_{sh} : Series and shunt resistance (Ω), q: electron charge (1.60217*10-19 C), N_s: number of cells in series.

The simulation parameters of the Sun power SPR-305-WHT PV module are listed in Table. 1

Table. 1 PV module parameter

Description	Rating
Maximum power (P_{MP})	305 W
Maximum current (I_{MP})	5.58 A
Maximum voltage (V_{MP})	54.7 V
Short circuit current (I_{SC})	5.96 A
open circuit voltage (V_{oc})	64.2 V
Temperature (T)	25^0C
Irradiations (R)	1000 W/m^2
No. of PV Cells in series	8

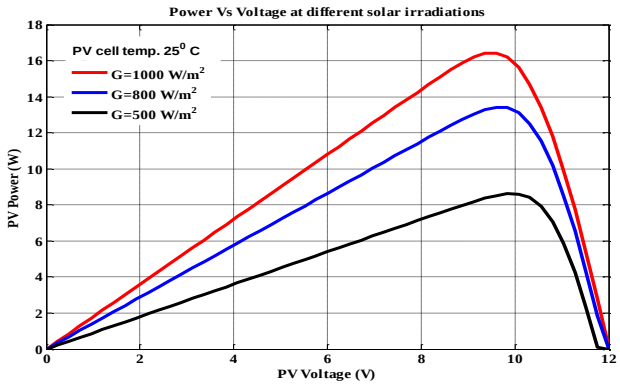

(a)

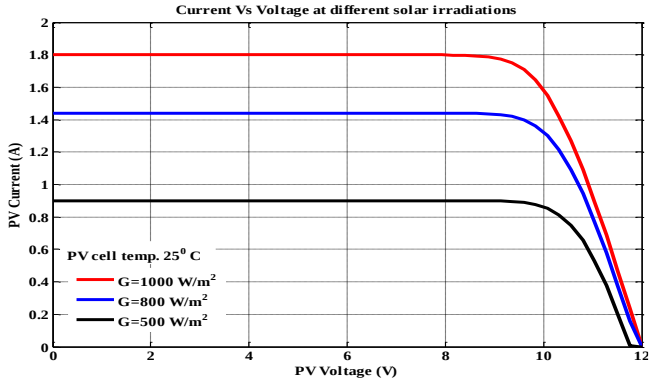

(b)

Fig. 2 Solar cell characteristics at different irradiation conditions, (a) P-V characteristics, (b) I-V characteristics

The variations in P-V and I-V characteristics of solar cell at constant temperature of 25^0 C and different irradiation conditions of 500 W/m^2, 800 W/m^2 and 1000 W/m^2 is shown in Fig. 2. From the literature [8], solar irradiation continuously varies, then the correspondingly output power of the solar cell is also variable. Understanding the problem, for obtaining the continuous and constant output, a DC-DC converter is required with MPPT control to maintain the DC link voltage to an optimum value.

2.1.1. Analysis of Cuk converter

PV panel unregulated output voltage is converted into a regulated voltage by using the Cuk converter as shown in Fig. 3. The energy transfer in cuk converter is associated with the capacitor, whereas in conventional converter it is associated with inductor. Thus it provides continuous input current. It is a type of chopper which gives the output voltage as negative with respect to common terminal and it operates in the continuous conduction mode [9].

In Fig. 3, when switch S_1 is turned ON, diode D_1 is reverse biased, and the current through inductor L_1 and inductor L_2 increase gradually and delivers power to the load. When switch S_1 is OFF, the diode becomes forward bias and the capacitor C_1 starts discharging for the next cycle. The Cuk converter DC output voltage in terms of the duty cycle ratio is given as follows in Eq. (2) [10,11].

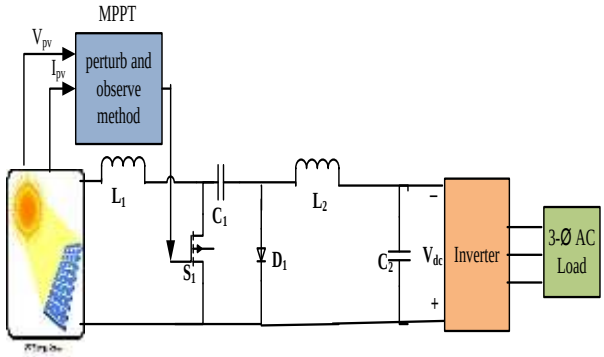

Fig. 3 PV system with Cuk converter

$$V_{cuk} = \left(\frac{d_1}{1-d_1}\right) V_{pv} \tag{2}$$

where: $d_1 = \dfrac{V_{cuk}}{V_{cuk} + V_{pv}}$ is duty ratio of Cuk converter, V_{cuk} is Cuk converter output voltage and V_{pv} is PV system output voltage.

2.1.2. MPPT Control algorithm for PV system

Perturb and observer (P&O) based MPPT technique is most commonly used controller to track the maximum available power from the PV system, because of its plain structure, less parameters and easy to implement [12].

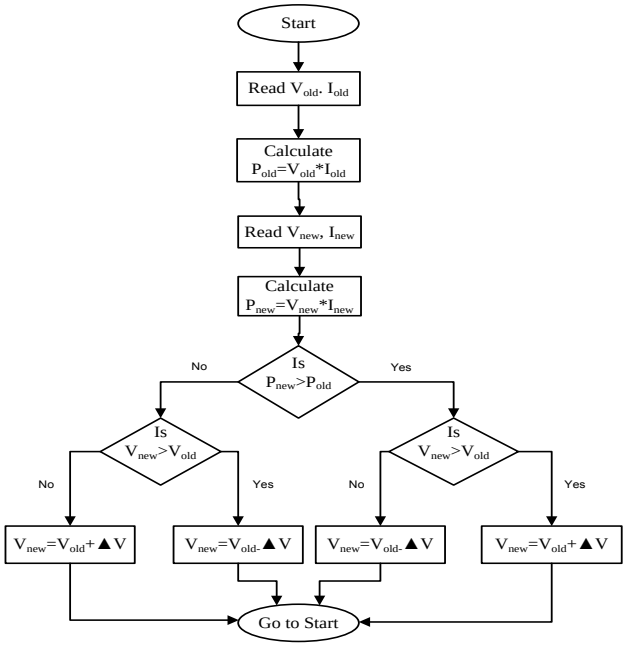

Fig. 4 Flow chart for perturbs and observes method [6]

The pictorial representation of P&O algorithm is shown in Fig.4 and the maximum power point is obtained by perturbing the PV array terminal voltage with respect to PV output power. If output power is increased, then the next cycle, the terminal voltage will be moved in a positive direction and vice versa [13].

2.2. *Wind energy conversion system*

The total power produced by the wind energy conversion system is strongly related to wind speed. The quadratic model [14,15] to calculate power produced is given in Eq. (3),

$$P_w(V_v)=\begin{cases} P_n\dfrac{V_v^2-V_d^2}{V_n^2-V_d^2} & ;V_d<V_v<V_n \\ P_n & ;V_n<V_v<V_c \\ 0 & ;V_v\le V_d \text{ and } V_v\ge V_c \end{cases} \quad (3)$$

where, P_w: wind turbine output power (KW), P_n: Nominal power (KW), V_d: Cut-in wind speed (m/s), V_n: Rated wind speed (m/s),V_s: Cut-off wind speed (m/s) and V_v: Wind speed (m/s).

A wind turbine has been modeled by an aerodynamic input torque, which drives a wind generator [16]. The mechanical output power P_m captured by the wind turbine is given as in Eq. (4) [17,18],

$$P_m=\frac{1}{2}C_p(\beta,\lambda)\rho\prod R^2V_v^3 \quad (4)$$

where, C_p: The rotor power coefficient, β: The blade pitch angle (degree), λ: The tip speed ratio, ρ: Air density (Kg/m3) and R: Wind blade radius (m).

The simulation parameters of PMSG based wind energy system [19] is listed in Table. 2

Table. 2 Parameters of wind system

Description	Rating
Power (P)	1.8 KW
Impedance (R_a)	0.775 Ω
Inductance (L_q and L_d)	7.31 mH
Magnetizing flux ($Ø_m$)	0.37387 wb
Torque/Current (T/A)	1.1216 Nm/A
Pair of poles (P_P)	2
Moment of inertia (J)	0.00126811 kg/m^2
Coefficient of friction (B)	0
Wind speed (N)	12 m/s

The characteristics of wind turbine power are shown in Fig. 5 which describes the total power captured by the turbine as a function of various wind speeds varied from 6 m/s to 12 m/s. When the wind speed changes, the generator rotor speed should track these changes in order to produce the maximum power from the available wind speed.

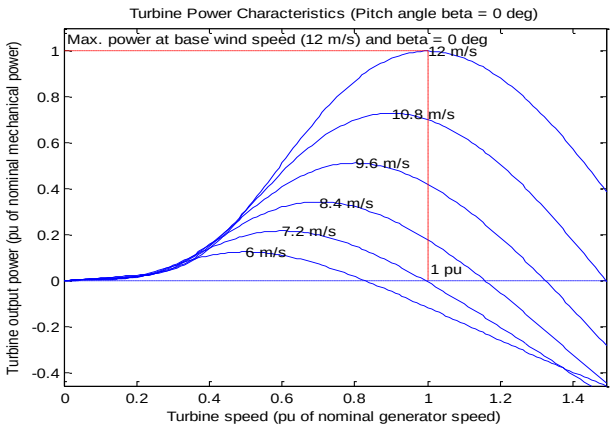

Fig. 5 Wind Turbine power characteristics

The wind energy system generates variable voltage and variable frequency power, which is not suitable for grid integration. This generated power is transferred to the grid/ standalone system by placing bidirectional back-back power converters between the wind generation system and grid/ standalone system. In this first converter, act as a rectifier for obtaining the regulated DC output power and then converted into AC by operating the second converter as inverter to meet the specifications of the grid/standalone system.

2.2.1. *Analysis of the SEPIC converter*

The rectified wind energy system output voltage is given as input to the single ended primary inductor converter (SEPIC) for obtaining desired voltage to meet the load demand as shown in Fig. 6. Basically SEPIC converter is a chopper; it gives either greater than or less than the input voltage. Here step up mode is considered to match the load profile. The DC output voltage of the SEPIC converter in terms of the duty cycle ratio is given as follows in Eq. (5) [10,11].

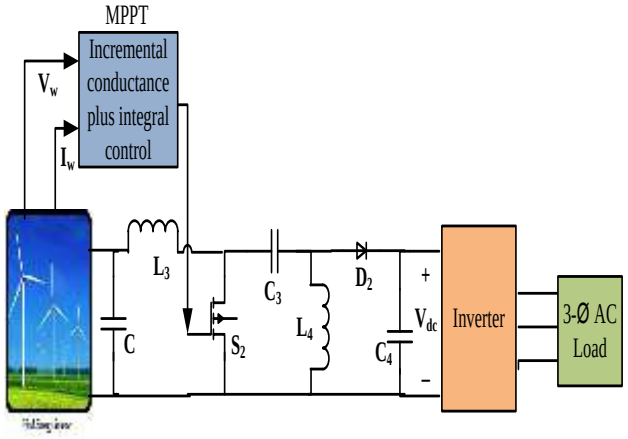

Fig. 6 Wind system with SEPIC converter

In Fig. 6, when switch S_2 is turned ON and diode D_2 is reverse biased then the current through inductor L_3 and inductor L_4 increases gradually and delivers power to the load. When switch S_2 is OFF, the diode becomes forward bias and capacitor C_3 starts discharging for the next cycle.

$$V_{sepic} = \left(\frac{d_2}{1-d_2}\right) V_{wind} \quad (5)$$

where, $d_2 = \frac{V_{sepic}}{V_{sepic} + V_{wind}}$ is the duty ratio of SEPIC converter, V_{sepic} is output voltage of SEPIC converter and V_{wind} is wind output voltage.

2.2.2. MPPT Control algorithm for wind system

To extract the maximum power from the wind, incremental conductance method is used. The pictorial representation of the incremental conductance method is shown in Fig. 7.

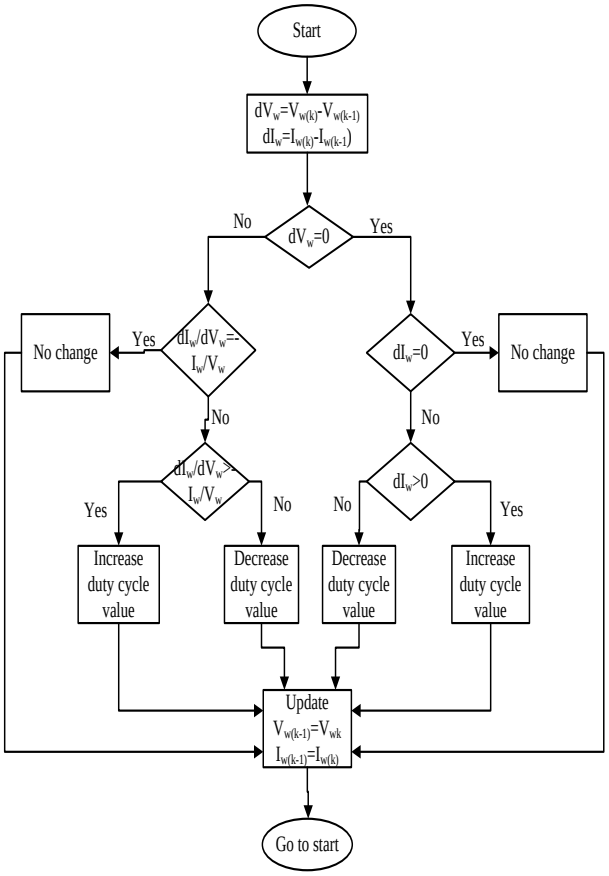

Fig. 7 Flow chart for Incremental conductance method [6]

The incremental conductance method tracks the maximum power based on the slope of the output power characteristics and integral controller to minimize the $\left(\frac{d_{I_w}}{d_{v_w}} + \frac{I_w}{V_w}\right)$ error. The maximum power point is obtained when the slope of the power curve is zero $\left(\frac{dP_w}{dV_w} = 0\right)$ or $\left(\frac{\Delta I_w}{\Delta V_w} = \frac{-I_w}{V_w}\right)$, the slope is positive when $\left(\frac{dP_w}{dV_w} > 0\right)$ or $\left(\frac{\Delta I_w}{\Delta V_w} > \frac{-I_w}{V_w}\right)$ the slope is negative when $\left(\frac{dP_w}{dV_w} < 0\right)$ or $\left(\frac{\Delta I_w}{\Delta V_w} < \frac{-I_w}{V_w}\right)$. Thus the maximum power point is obtained by comparing the instantaneous conductance $\left(\frac{I_w}{V_w}\right)$ to the incremental conductance $\left(\frac{\Delta I_w}{\Delta V_w}\right)$ [20,21].

2.3. Design of proposed converter for hybrid system

The schematic diagram of proposed integrated Cuk-SEPIC converter is shown in Fig. 8. The proposed integrated converter is designed by rearranging the diodes (D_1, D_2) in Cuk and SEPIC converter and by utilizing the output inductor L_2 of the Cuk converter by the SEPIC converter. It simplifies the power system circuit complexity and reduces the cost and size of the system. It is a three port converter, the first port is for connecting the input PV source, the second port is for connecting the wind source and the third port is output port for connecting output as input to the inverter to supply the 3-Ø AC power to the stand alone system.

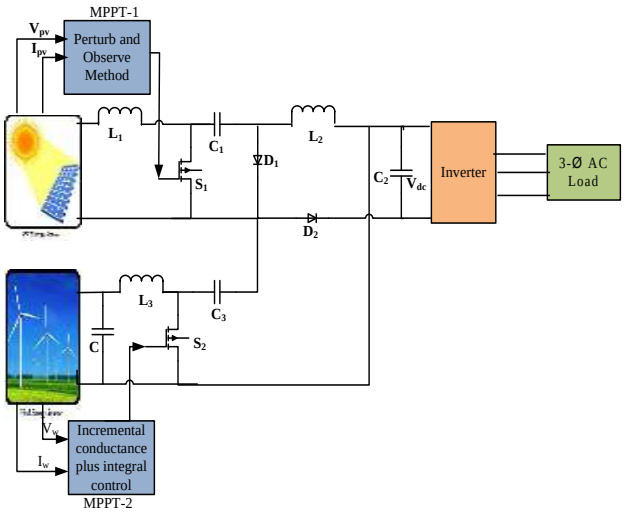

Fig. 8 Integrated Cuk-SEPIC converter

Based on the reconfiguration discussed above, each converter will operate simultaneously or individually upon the availability of PV and wind sources. The DC link voltage, V_{dc} of the proposed converter is the sum of two converters outputs as shown in Eq. (6) and it is maintained constant by varying the duty cycle d_1 and d_2 of Cuk and SEPIC converters which are obtained from the Eq. (2) and Eq. (5) respectively by using duty ratio control.

$$V_{dc} = \left(\frac{d_1}{1-d_1}\right) V_{pv} + \left(\frac{d_2}{1-d_2}\right) V_{wind} \quad (6)$$

Due to the alternative nature of both solar and wind sources vary continuously. MPPT control algorithms play a vital role in renewable energy sources application to obtain

maximum power and efficiency. There is a huge amount of maximum power control algorithms and they differ from each other based on the sensors requirement, complexity, cost, convergence speed, effectiveness range, behavior of the algorithm when input parameter changes and implementation of hardware [22-24]. For the proposed system, perturb and observe method and Incremental conductance plus integral control methods are used for extracting the maximum power.

3. Power Conversion Analysis of Proposed Converter

Based on the availability of renewable energy source, the power semiconductor switches (S_1 for PV and S_2 for Wind) present in proposed converter shown in Fig. 9 changes its status from ON/OFF and operates in various modes as explained below:

Mode-I: S_1-ON, S_2-ON (Both sources available)

In mode-I, both PV and wind system together generates power to meet the load demand.

$$I_{L1} = I_{PV} + \frac{V_{PV}}{L_1} t \tag{7}$$

$$I_{L2} = I_{dc} + \frac{V_{C1} + V_{C3}}{L_2} t \tag{8}$$

$$I_{L3} = I_W + \frac{V_W}{L_3} t \tag{9}$$

where, I_{dc} is the DC link current (A).

The equivalent circuit for both the switches S_1 and S_2 are ON is shown in Fig. 9(a). In this mode D_1 and D_2 are in reverse bias. During the period d_1 and d_2, shown in Fig. 10 L_1 is charged by PV source, L_3 is charged by Wind source and the energy stored in capacitors C_1 and C_3 starts discharging to the capacitor C_2 through the inductor L_2. The mathematical equations of inductor currents L_1, L_2 and L_3 are shown in Eq. (7), (8) and (9) respectively.

Mode-II: S_1-ON, S_2-OFF (Only PV available)

In mode-II, only PV source is available to generate power to meet the load demand.

$$I_{L1} = I_{PV} + \frac{V_{PV}}{L_1} t \tag{10}$$

$$I_{L2} = I_{dc} + \frac{V_{C1}}{L_2} t \tag{11}$$

$$I_{L3} = I_W + \frac{V_W - V_{C3}}{L_3} t \tag{12}$$

The equivalent circuit for switches S_1 ON and S_2 OFF is shown in Fig. 9(b). In this mode D_1 is reverse bias and D_2 is in forward bias. During the period d_1, shown in Fig. 10 L_1 is charged by PV source, the capacitors C_1 starts discharging the stored energy to the inductor L_2. D_2 provides the closed path to discharge the stored energy in L_3 and C_3 to the Capacitor C_2. The mathematical equations of inductor currents L_1, L_2 and L_3 are shown in Eq. (10), (11) and (12) respectively.

Mode-III: S_1-OFF, S_2-ON (Only wind available)

In mode-III only wind source is available for power generation.

$$I_{L1} = \frac{V_{PV} - V_{C1}}{L_1} t + I_{PV} \tag{13}$$

$$I_{L2} = I_{dc} - \frac{V_{C3}}{L_2} t \tag{14}$$

$$I_{L3} = I_W + \frac{V_W}{L_3} t \tag{15}$$

The equivalent circuit for switches S_1 OFF and S_2 ON is shown in Fig. 9(c). In this mode D_1 is forward bias and D_2 is in reverse bias condition. During the period d_2, as shown in Fig. 10, L_3 is charged by Wind source and the L_1 is charged by the capacitors C_1. D_1 provides the closed path to charge the L_2 by discharging the Capacitor C_3. The mathematical equations of inductor currents L_1, L_2 and L_3 are shown in Eq. (13), (14) and (15) respectively.

Mode-IV: S_1-OFF, S_2-OFF (Both sources are not available)

In mode-IV both sources are not available, this is very rare case because both PV and wind system are complement nature. So this case is not considered in the analysis of proposed converter.

$$I_{L1} = I_{PV} + \frac{V_{PV} - V_{C1}}{L_1} t \tag{16}$$

$$I_{L2} = I_{dc} \tag{17}$$

$$I_{L3} = I_W + \frac{V_W - V_{C3}}{L_3} t \tag{18}$$

The equivalent circuit for both switches S_1 and S_2 are OFF is shown in Fig. 9(d). In this mode D_1 and D_2 are in forward bias condition. During the period $(1\text{-}d_2)$ shown in Fig. 10 D_2 provides a path for charging the L_3 by the capacitor C_3 and D_1 provides a path for charging the L_1 by the capacitors C_1 and the energy stored in the inductor L2 is transferred to the capacitor C_2. The mathematical equations of inductor currents L_1, L_2 and L_3 are shown in Eq. (16), (17) and (18) respectively. The summary of the proposed Cuk-SEPIC converter modes of operation with switching states are listed in Table 3.

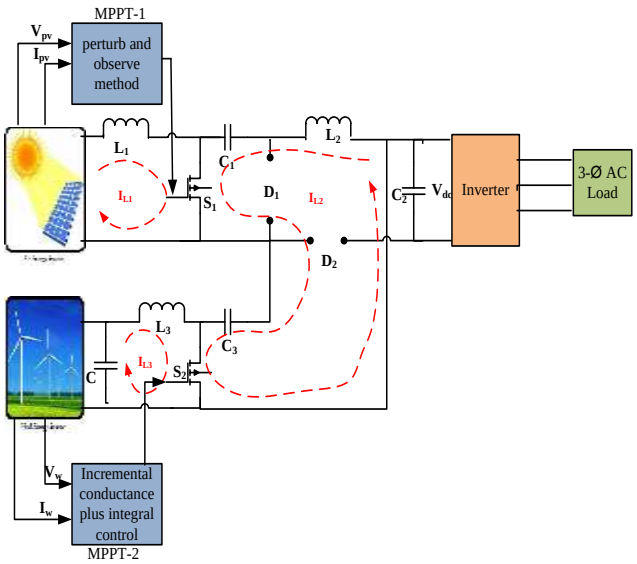

(a) Mode-I: S_1-ON, S_2-ON (Both sources available)

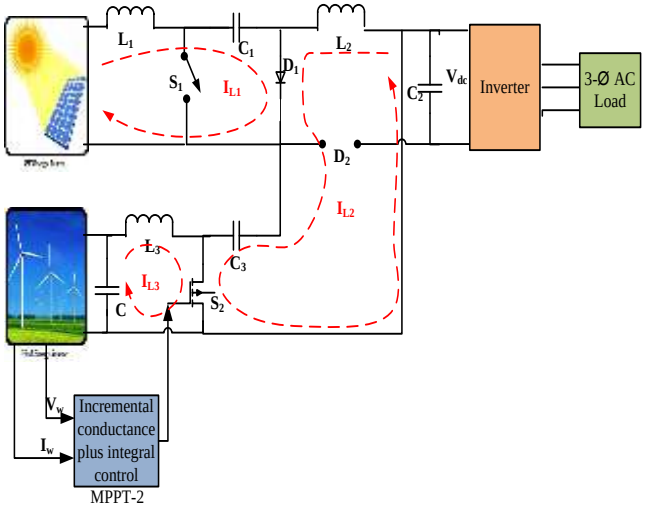

(c) Mode-III: S_1-OFF, S_2-ON (Only wind available)

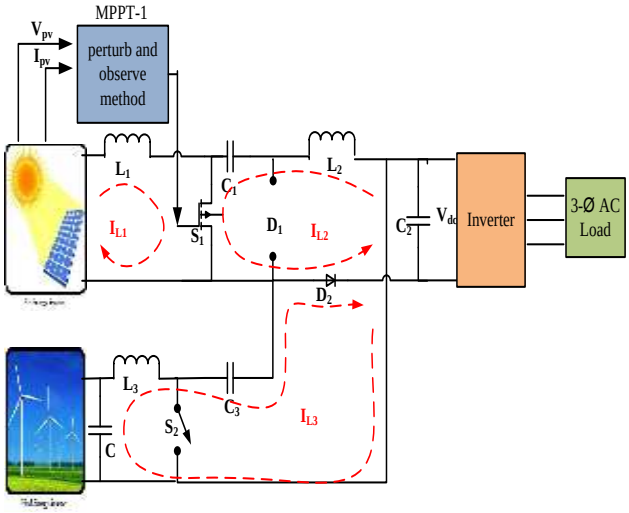

(b) Mode-II: S_1-ON, S_2-OFF (Only PV available)

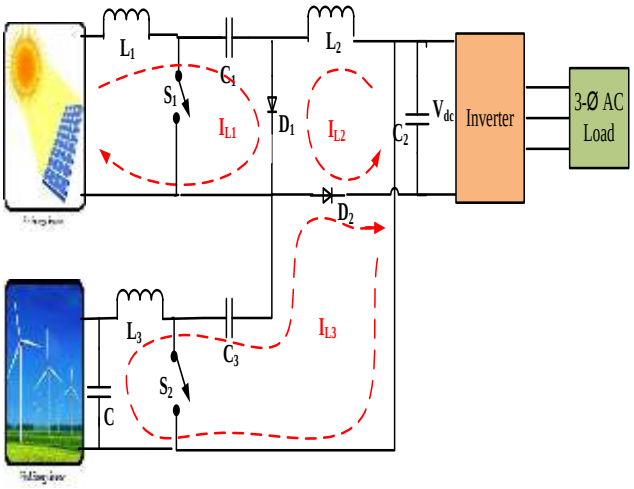

(d) Mode-IV: S_1-OFF, S_2-OFF (Both sources are not available)

Fig. 9 Modes of operation proposed converter

Table. 3 Switching states of proposed Cuk-SEPIC converter

Mode of operation	PV source	Wind source	Switch, S_1	Switch, S_2	D_1	D_2	Charging and discharging		
							L_1	L_2	L_3
I	Available	Available	ON	ON	Reverse bias	Reverse bias	PV source	C_1 & C_3	Wind source
II	Available	Unavailable	ON	OFF	Reverse bias	Forward bias	PV source	C_1	C_3
III	Unavailable	Available	OFF	ON	Forward bias	Reverse bias	C_1	C_3	Wind source
IV	Unavailable	Unavailable	OFF	OFF	Forward bias	Forward bias	C_1	C_2	C_3

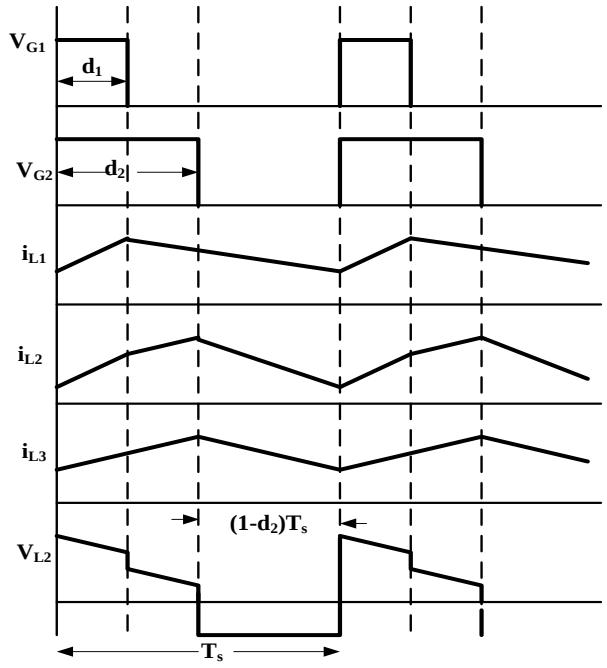

Fig. 10 Cuk-SEPIC converter inductor waveforms

4. Implementation Results

The proposed topology is implemented in Matlab/Simulink to validate the converter performance. The input solar irradiations and wind speed are considered as a constant and continuously varies with time as shown in Fig. 11 and the parameter specifications of the proposed hybrid system is listed in Table 4.

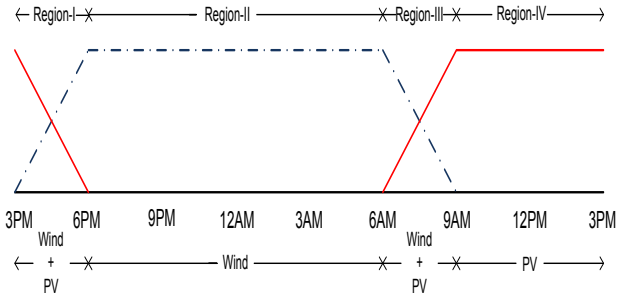

Fig. 11 Availability of PV and wind source in a day

Table. 4 Parameter specifications of the hybrid system

Description	Ratings
PV rating	440V, 4.5A and 2KW
Wind rating	400V, 4.5A and 1.8KW
Cuk converter parameters	L_1=0.045H, C_1=2.96e-6F
SEPIC converter parameters	L_3=0.045H, C_3=2.96e-6F
Sharing inductor	L_2=0.03H
DC link capacitor	C_2=2.96e-8F
Load resistance	R=95Ω
Switching frequency	20 kHz

In region-I (3PM to 6PM), both PV and wind sources of hybrid system are available and varies continuously with respect to time as per the consideration of availability of energy sources. The proposed converter operates in mode-I in this region. In mode-1, the converter output voltage is the sum of the PV and wind output voltages, the average voltage obtained in this region is 428V. The loss in voltage is due to the transition between the sources. The solar irradiation starts decreasing where as the wind speed starts increasing, then the corresponding outputs of both the energy sources are added to meet the load demand.

In region-II (6PM to 6AM), wind source is the only available energy source. Here the proposed converter operates in mode-III and transfers generated power from source to load. The available wind energy source is sufficient to meet the load demand as per the consideration of availability of energy sources. The output voltage obtained in this region is 440V which is the full wind capacity voltage.

In region-III (6AM to 9AM), both PV and wind sources of hybrid system are available and varies continuously with respect to time as per the consideration of availability of energy sources. The proposed converter operates in mode-I in this region. The wind speed starts decreasing where as the PV source irradiation starts increasing, then the corresponding outputs of both the sources are added to meet the load demand. This region-III is same as region-I. The voltage in this region drops to 428V.

In region-IV (9AM to 3PM), PV is the only available energy source. Here the proposed converter operates in mode-II and transfers generated power from source to load. The available PV source is sufficient to meet the load demand as per the consideration of availability of energy sources. The load voltage in this region is entirely relay on PV source which is 440V.

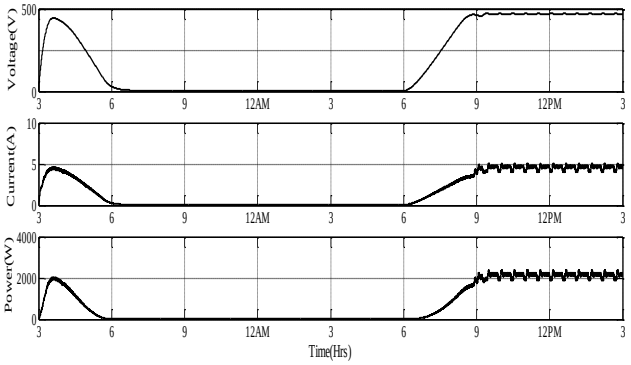

Fig. 12 Simulated output voltage, current and power from PV source

As per the consideration of the availability of solar irradiations as shown in Fig.11, PV panel starts generating power at 6AM and reaches rated capacity at 9AM (region-III) after that it generates constant power up to 3PM (region-IV) and then starts decreasing the generating power gradually up to 6PM (region-I) as clearly shown in Fig. 12. Similarly, wind energy system starts generating power at 3PM and reaches rated capacity at 6PM (region-I) after that it generates constant power up to 6AM (region-II) and then

starts decreasing the generating power gradually up to 9AM (region-III) as clearly shown in Fig. 13.

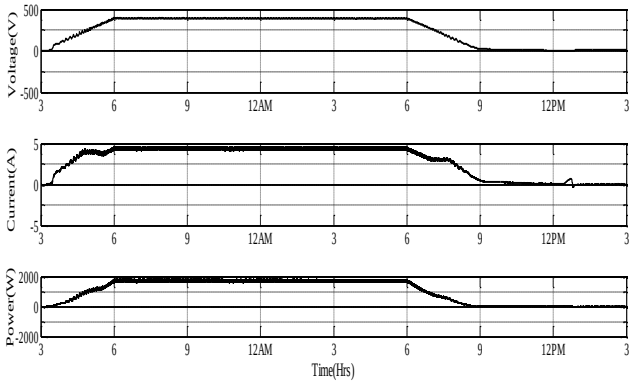

Fig. 13 Simulated output voltage, current and power from Wind source

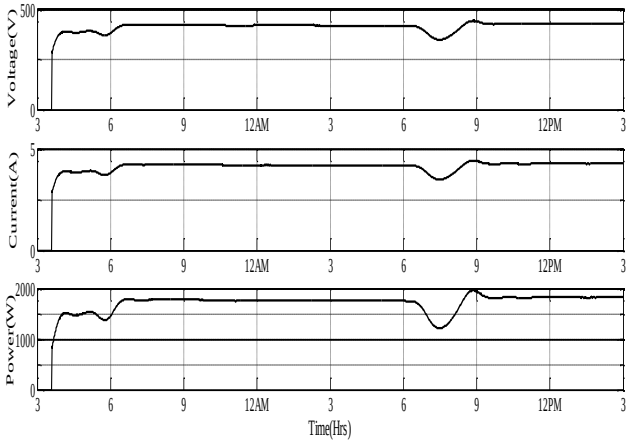

Fig. 14 Simulated DC link voltage, current and power

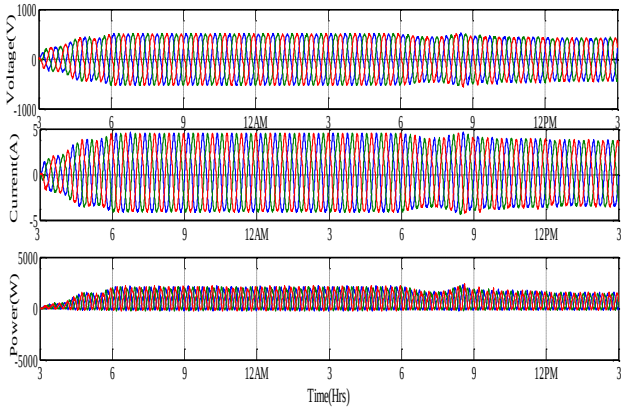

Fig. 15 Simulated inverter output voltage, current and power

During 6AM to 6PM (region-II), wind system with SEPIC converter provides constant power to the load and from 9AM to 3PM (region-IV), PV system with Cuk converter provides constant power to meet the load demand. But from 6AM to 9AM (region-III) and 3PM to 6PM(region-I) both wind and PV sources are available and continually varied oppositely due to its complementary nature, then the proposed converter operates in simultaneous mode and add the output of two sources and fed to the load. The constant DC link voltage is maintained by operating the proposed converter in individual and simultaneous modes as shown in Fig. 14. The constant DC link voltage V_{dc} is fed to the 3-Ø inverter with PWM control switching technique for obtaining 3-Ø 440V AC supply throughout the day for the stand alone application as in Fig. 15. The total harmonic distortion (THD) of inverter voltage is measured as 5.39%, and it is shown in Fig. 16.

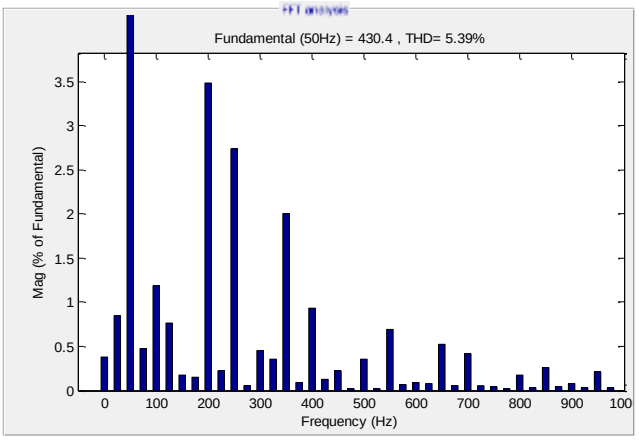

Fig. 16 Inverter output voltage THD spectrum

The summary of the proposed converter modes of operation during a day, with availability of source and corresponding output voltages is listed in Table. 5.

5. Conclusion

The analysis of integrated Cuk-SEPIC converter with MPPT has been presented for integration of hybrid PV and wind sources. In this paper two separate DC-DC converters are merged together in order to minimize the converter components, size and complexity. The proposed system does not use any additional input filters for the elimination of high frequency harmonics and to improve the converter efficiency. Since, less number of switching devices and passive components are used in this system it reduces the cost and complexity of the overall system. The operation of the proposed converter depends on the control of two switches (S_1 and S_2) which simplifies the control circuit, becomes economical and it doesn't require any supervisory control for switching purposes. MPPT has been realized for both PV and wind sources by using perturb and observe method and Incremental conductance plus integral control method respectively. The developed converters make the use of natural complementary behaviour of PV and wind system and maintain constant DC link voltage of 440V throughout the day. The simulation results of the proposed model are presented in three operating regions (both PV and wind sources are available, only PV source available and only wind source is available).

Table. 5 Modes of operation during a day

Region	Time (Hrs)	PV source	Wind source	Mode of operation	Output voltage, V_{dc}
I	3 PM to 6 PM	Available	Available	I	$\left(\frac{d_1}{1-d_1}\right)V_{pv}+\left(\frac{d_2}{1-d_2}\right)V_{wind}$
II	6 PM to 6 AM	Unavailable	Available	III	$\left(\frac{d_2}{1-d_2}\right)V_{wind}$
III	6 AM to 9 AM	Available	Available	I	$\left(\frac{d_1}{1-d_1}\right)V_{pv}+\left(\frac{d_2}{1-d_2}\right)V_{wind}$
IV	9 AM to 3 PM	Available	Unavailable	II	$\left(\frac{d_1}{1-d_1}\right)V_{pv}$

References

[1] Xiong Liu, Poh Chiang Loh, Peng Wang, and Frede Blaabjerg, "A direct power conversion topology for grid integration of hybrid AC/DC energy resources", IEEE Transactions on Industrial Electronics, vol. 60, no. 12, pp. 5696-5707, 2013.

[2] Neng Zhang, Danny Sutanto, and Kashem M. Muttaqi, "A review of topologies of three-port DC–DC converters for the integration of renewable energy and energy storage system", Renewable and Sustainable Energy Reviews, vol. 56, pp. 388-401, 2016.

[3] Akar, Furkan, et al. "A Bidirectional Non-Isolated Multi Input DC-DC Converter for Hybrid Energy Storage Systems in Electric Vehicles", IEEE Transactions on Vehicular Technology, vol. 65, no. 10,pp. 7944-7955, October 2016.

[4] Jayalakshmi, N. S., D. N. Gaonkar, and Pramod Bhat Nempu, "Power Control of PV/Fuel Cell/Supercapacitor Hybrid System for Stand-alone Applications", International Journal of Renewable Energy Research (IJRER) , vol. 6.2, pp. 672-679, 2016.

[5] Murugesan, Karthik, and Vijayachitra Senniappan, "Dynamic Modeling and Analysis of Power Sharing Control Strategy Based Fuel Cell/Battery Assisted Hybrid Electric Vehicle System", International Journal of Renewable Energy Research (IJRER), vol. 5.1, pp. 139-150, 2015.

[6] S. Saravanan, and Ramesh Babu N, "Maximum power point tracking algorithms for photovoltaic system–A review", Renewable and Sustainable Energy Reviews, vol. 57, pp. 192-204, 2016.

[7] Ersan Kabalci, "Design and analysis of a hybrid renewable energy plant with solar and wind power", Energy Conversion and Management, vol. 72, pp. 51-59, 2013.

[8] S. Saravanan, and Ramesh Babu N, "RBFN based MPPT algorithm for PV system with high step up converter", Energy Conversion and Management, vol. 122, pp. 239-251, 2016.

[9] Maria Bella Ferrera, Salvador P. Litran, Eladio Duran Aranda, and Jose Manuel Andujar Marquez, "A Converter for Bipolar DC Link Based on SEPIC-Cuk Combination", IEEE Transactions on Power Electronics, vol.30, no.12, pp. 6483-6487, 2015.

[10] Shagar Banu M, Vinod .S, and Lakshmi. S, "Design of DC-DC converter for hybrid wind solar energy system", International Conference on Computing, Electronics and Electrical Technologies [ICCEET], pp. 429-435, 2012.

[11] Sajib Chakraborty, S M Salim Reza, Wahidul Hasan, "Design and analysis of hybrid solar-wind energy system using CUK & SEPIC converters for grid connected inverter application", IEEE 11th International Conference on Power Electronics and Drive Systems (PEDS), pp. 278-283, 9–12 June 2015.

[12] Mukesh Kumar Gupta, and Rohit Jain, "MPPT simulation with DC submersible solar pump using output sensing direct control method and cuk converter", International Journal of Renewable Energy Research (IJRER), vol.3, no.1, pp. 186-191, 2013.

[13] Jubaer Ahmed,and Zainal Salam, "An improved perturb and observe (P&O) maximum power point tracking (MPPT) algorithm for higher efficiency", Applied Energy, vol. 150, pp. 97-108, 2015.

[14] Salwan S. Dihrab, and K. Sopian, "Electricity generation of hybrid PV/wind systems in Iraq", Renewable Energy, vol. 35, pp. 1303-1307, 2010.

[15] Fazia Baghdadi, Kamal Mohammedi, Said Diaf, and Omar Behar, "Feasibility study and energy conversion analysis of stand-alone hybrid renewable energy

system", Energy Conversion and Management, vol. 105, pp. 471-479, 2015.

[16] Kaushik Das, Anca D Hansen and Poul E Sørensen, "Understanding IEC standard wind turbine models using SimPowerSystems", Wind Engineering, vol. 40(3), pp. 212-227, Jun 2016.

[17] Ramji Tiwari, and Ramesh Babu. N, "Fuzzy Logic Based MPPT for Permanent Magnet Synchronous Generator in wind Energy Conversion System", IFAC-Papers Online, vol. 49.1, pp. 462-467, 2016.

[18] Jayalakshmi, N. S., and D. N. Gaonkar, "Operation of Grid Integrated Wind/PV Hybrid System with Grid Perturbations", International Journal of Renewable Energy Research (IJRER), vol.5, no.4, pp. 1106-1111, 2015.

[19] Ting, Naim Suleyman, et al. "Comparison of SVPWM, SPWM and HCC control techniques in power control of PMSG used in wind turbine systems", 2015 Intl Aegean Conference on Electrical Machines & Power Electronics (ACEMP), 2015 Intl Conference on Optimization of Electrical & Electronic Equipment (OPTIM) & 2015 Intl Symposium on Advanced Electromechanical Motion Systems (ELECTROMOTION) IEEE, pp. 69-74, 2015.

[20] Tiwari Ramji, and N. Ramesh Babu. "Recent developments of control strategies for wind energy conversion system", Renewable and Sustainable Energy Reviews, vol. 66, pp. 268-285, 2016.

[21] Ali Q. Al-Shetwi, Muhamad Zahim Sujod, A. Al Tarabsheh, and Ibrahim A. Altawil, "Design and Economic Evaluation of Electrification of Small Villages in Rural Area in Yemen Using Stand-Alone PV System", International Journal of Renewable Energy Research (IJRER), vol.6, no.1, pp. 289-298, 2016.

[22] Mustafa Engin Başoğlu, and Bekir Çakır, "Comparisons of MPPT performances of isolated and non-isolated DC–DC converters by using a new approach", Renewable and Sustainable Energy Reviews, vol. 60, pp. 1100-1113, 2016.

[23] Joanne Hui, Alireza Bakhshai, and Praveen K. Jain, "A hybrid wind-solar energy system: A new rectifier stage topology", Applied Power Electronics Conference and Exposition (APEC), pp. 155-161, 2010.

[24] Sajib Chakraborty, M. A. Razzak, Md. Sarwar Uddin Chowdhury, and Sudipta Dey, "Design of a transformer-less grid connected hybrid photovoltaic and wind energy system", The 9th International Forum on Strategic Technology (IFOST), pp. 400-403, 21-23 October 2014.